

# Conversion electron Mössbauer spectroscopy studies of ultrathin Fe films on MgO(001)

M. Zając<sup>a</sup>, K. Freindl<sup>b</sup>, K. Matlak<sup>a</sup>, M. Ślęzak<sup>a</sup>, T. Ślęzak<sup>a,b</sup>,  
N. Spiridis<sup>b</sup>, J. Korecki<sup>a,b,\*</sup>

<sup>a</sup> Faculty of Physics and Applied Computer Science, AGH University of Science and Technology, al. Mickiewicza 30, 30-059 Kraków, Poland

<sup>b</sup> Institute of Catalysis and Surface Chemistry, Polish Academy of Sciences, ul. Niezapominajek 8, 30-239 Kraków, Poland

Available online 22 April 2007

## Abstract

The initial growth and influence of annealing on structural and magnetic properties of 5 monolayers epitaxial Fe films on cleaved and polished MgO(001) substrates was studied using conversion electron Mössbauer spectroscopy (CEMS). Broadening of LEED spots indicated a granular structure of the films grown at room temperature. The CEMS analysis showed that the film on the cleaved substrate is flat and consists of a 2 ML interfacial layer with the electronic structure affected by the oxidic substrate, while the remaining 3 ML are metallic with the Curie temperature below RT. Annealing changes the film structure, as seen by CEMS, but only for temperatures above 550 K. In the annealing process the continuous film breaks into 3-dimensional islands and oxidation takes place at the Fe/cleaved–MgO interface. On the polished substrate, the as-prepared film consists of small superparamagnetic metallic iron particles. Contrary to the cleaved substrate, no oxidation is observed at the interface upon annealing.

© 2007 Elsevier B.V. All rights reserved.

**Keywords:** Iron; Magnesium oxide; Growth; Epitaxy; Magnetic films; Mössbauer spectroscopy

## 1. Introduction

Iron films on MgO have attracted a lot of attention for their importance in basic research as well as in technological applications [1]. Fe monolayers on MgO are considered prototypic 2-dimensional magnets [2], ultrathin epitaxial films are used as seed and buffer layers in the epitaxial growth of different metals [3,4], and they have been applied in tunneling magnetoresistive devices with spectacular results [5]. While the growth and structure of Fe films with the thickness warranting their electrical continuity (above 1 nm), suitable for STM measurement is well known (for

review see [1]), only a few papers deal with structural [6–10] and especially magnetic [11–13] properties of sub-nanometer films. Theoretical predictions of the strongly enhanced ground state magnetic moments in Fe mono- and bi-layers,  $3.07 \mu_B$  and  $2.9 \mu_B$ , respectively, that are close to the value for a freestanding Fe layer ( $3.1 \mu_B$ ) [2] have been never confirmed experimentally for ultrathin Fe films, probably due to a deviation from flat growth [13]. An enhancement of the Fe magnetic moment was observed for an Fe monolayer in contact with MgO (the Fe monolayer was deposited on a thicker Co film) [14] but ultrathin iron films on MgO have been found to be ferromagnetic with a magnetic moment very similar to that of bulk Fe [11]. There is no data on the Curie temperature, probably because the magnetic transition is masked by superparamagnetism that often dominates the magnetic behavior for discontinuous films, being for this system a consequence of Schwöbel barriers [15]. The film morphology depends on the preparation temperature but also on substrate defects that determine the nucleation process [16].

\* Corresponding author. Address: Faculty of Physics and Applied Computer Science, AGH University of Science and Technology, al. Mickiewicza 30, 30-059 Kraków, Poland. Tel.: +48 12 617 2911; fax: +48 12 634 1247.

E-mail address: [korecki@uci.agh.edu.pl](mailto:korecki@uci.agh.edu.pl) (J. Korecki).

The aim of the present paper is to study structural and magnetic properties of ultrathin Fe films with the emphasis on the Fe/MgO interface. For that purpose a film thickness of 5 monolayers (MLs) was chosen. Such a thickness ensured high contribution of the interface to measured properties and, on the other hand, secured coalescence of the growing film.

By use of conversion electron Mössbauer spectroscopy (CEMS) the analysis is site selective, i.e. magnetic properties of Fe atoms at different chemical and structural positions can be distinguished. Moreover, the evolution of Fe film properties upon annealing is discussed. In particular, differences between Fe films deposited on cleaved and polished MgO substrates are emphasized.

## 2. Experimental procedures

The samples were prepared and characterized in a multi-chamber UHV system with the base pressure below  $1 \times 10^{-10}$  mbar. The system was equipped with a load-lock facility, a universal sample mounting and transfer system, standard surface characterization methods (a 4-greed electron optics for LEED and AES), a MBE system for deposition of several metals including  $^{56}\text{Fe}$  and  $^{57}\text{Fe}$  isotopes and a CEMS spectrometer.

All samples were deposited on MgO(001) substrates, cleaved *ex situ* prior to the introduction into the UHV system or on polished ones. The substrates were UHV annealed at 800 K for several hours. For the cleaved substrates, such treatment resulted in a clean surface showing only traces of carbon contamination and a perfect background-free  $1 \times 1$  LEED pattern. On the contrary, commercial polished substrates always showed a pronounced carbon signal in the Auger spectra, with the intensity only an order of magnitude less than the oxygen line.

Fe was deposited from BeO crucibles heated by wrap-around tungsten coils. The crucible assemblies were embedded in a water-cooled shroud and the pressure during the deposition was maintained in the low  $10^{-10}$  mbar range. The film thickness was controlled during the deposition by quartz thickness monitors with an accuracy of about 0.2 ML. All 5 ML (7.2 Å)  $^{57}\text{Fe}$  films were deposited on substrates kept at RT.

*In situ* Mössbauer measurements were performed using an efficient 80–500 K CEMS spectrometer based on channeltron detection, with a 100 mCi  $^{57}\text{Co}(\text{Rh})$  source. The spectrometer geometry settled a fixed angle of  $45^\circ$  between the direction of the  $\gamma$ -ray propagation and the sample normal. The spectra were analyzed numerically by fitting a hyperfine field distribution (HFD) using the Voigt-lines based method of Rancourt and Ping [17]. In the method, the HFD is constructed by a sum of Gaussian components for the magnetic hyperfine field  $B_{\text{hf}}$ , isomer shift (IS) and quadrupole splitting (QS) distributions. Only linear correlations between  $B_{\text{hf}}$  and IS or QS can be used in the numerical procedure, which may lead to oversimplification and systematic error when a broad range of  $B_{\text{hf}}$  is analyzed.

The number of Gaussian components was increased gradually, such that a minimum number of fitting parameters were introduced. Once a statistically ideal fit was obtained, increasing the number of the component did not change the distribution or any of the essential fit parameters.

The Fe films were characterized *in situ* by low energy electron diffraction (LEED). LEED patterns showed an epitaxial growth of (001) oriented films with in-plane crystallographic relations: Fe[100]/MgO[110]. Broadened LEED spots indicated imperfect growth: nucleation of small islands resulted in granular film structures. There was no apparent difference in the LEED patterns for the films grown on cleaved and polished substrates.

## 3. CEMS results and discussion

CEMS spectra for the 5 ML Fe film on the cleaved substrate are shown in Fig. 1. A room temperature (RT) spectrum for the as-prepared sample (Fig. 1a) reveals an unresolved asymmetric doublet structure that becomes magnetically split at 80 K (Fig. 1b). By virtue of the spectral character (unresolved lines, relatively broad HFDs), the numerical fits are to some extent ambiguous, and different sets of the hyperfine parameters could give fits of a comparable quality. For that reason the spectra for the same sample taken at different temperatures were fitted simultaneously within a single model, in which spectral components were identified by their isomer shift values, which are good fingerprints of the chemical state of a  $^{57}\text{Fe}$  atom in a particular lattice site. It is interesting to note that lowering the temperature of a CEMS measurement from 300 K to 80 K results in a shift of the spectrum centroid to a more positive value due to a second order Doppler by about 0.12 mm/s [18]. Both spectra for the as-prepared film could be fitted consistently with two components, identified by their different IS values, as summarized in Table 1, which contains the fit results for the cleaved substrate. The component with IS close to the one of metallic Fe (labelled *M*), which is a single line at RT, reveals a complex structure at 80 K, splitting into three sub-components with the magnetic hyperfine field  $B_{\text{hf}}$  ranging from 33.8 T (the  $\alpha$ -Fe value) down to 10 T, with HFD becoming very broad for the small  $B_{\text{hf}}$  sub-component. This “metallic” component constitutes 60% of the total spectral intensity, which corresponds to contributions from 3 monolayers and is distributed almost equally over three sub-components. The component identified at RT with the high positive isomer shift (IS = 0.40 mm/s), labelled *I*, is a doublet, which splits magnetically at 80 K to a HFD site with  $B_{\text{hf}} = 29.7$  T and contributes to 40% of the total spectral intensity. The CEMS analysis leads us to the following model: three of five film monolayers have metallic iron properties – these atoms are located at the film surface, sub-surface and centre. Two remaining monolayers come form the Fe/MgO interface. The oxygen proximity and broken translational symmetry account for the high isomer shift

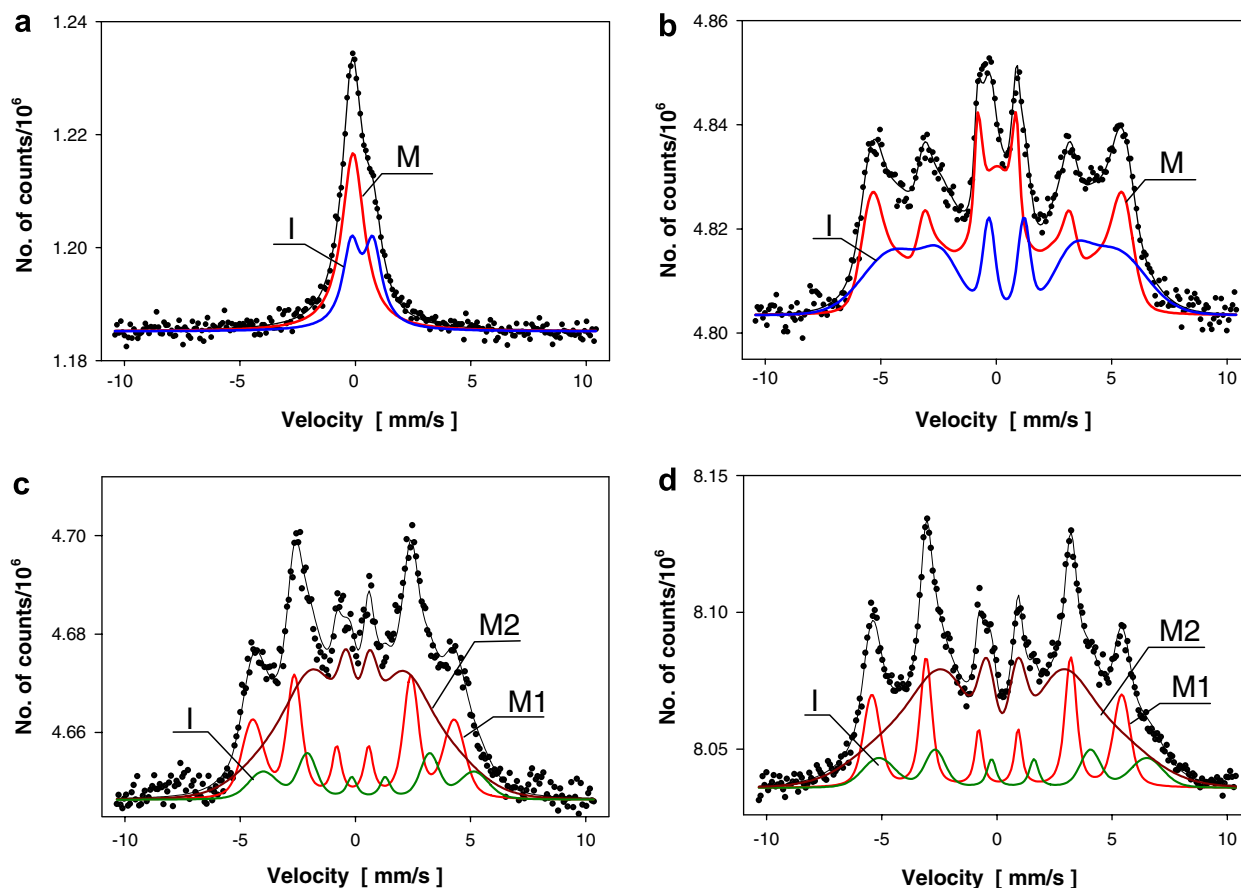


Fig. 1. *In situ* CEMS spectra of 5 ML  $^{57}\text{Fe}$  films on the cleaved MgO(001) substrate: (a) and (b) as prepared, measured at 300 K and 80 K, respectively; (c) and (d) after 1 h annealing at 570 K, measured at 300 K and 80 K, respectively. Symbols that identify the fitted component refer to Table 1.

Table 1  
Fitted hyperfine parameters for 5 nm  $^{57}\text{Fe}$ (001) films on the cleaved MgO(001) substrate

Sample/temperature (K)		IS (mm/s)	$B_{\text{hf}}$ (T)/ $\Delta B_{\text{hf}}$ (T) Subcomponents	QS (mm/s)	Relative intensity (%) Subcomponents					
As prepared	300	<i>M</i>	0.02(2)	–	0.00 (1)	59(3)				
		<i>I</i>	0.40(3)	–	$\pm 0.47(8)$	41(3)				
	80	<i>M</i>	0.14(2)	33.8(3)/2.4	27.9(4)/4.3	10.0(5)/11	0.00(2)	20(3)	16(3)	24(3)
		<i>I</i>	0.51(5)	29.7(5)/8.0	–	–	–0.04(3)	40(5)		
Annealed @ 570 K	300	<i>M1</i>	0.01(2)	27.1(2)/2.2	–	0.02(2)	28(5)			
		<i>M2</i>	0.24(2)	19.3(7)/9.4	–	0.02(4)	59(5)			
		<i>I</i>	0.67(5)	28.4(7)/3.2	–	0.00(5)	13(4)			
	80	<i>M1</i>	0.13(2)	33.6(1)/1.7	–	–0.04(2)	24(5)			
		<i>M2</i>	0.33(4)	26.1(8)/11.4	–	0.00(3)	63(5)			
		<i>I</i>	0.79(5)	36.0(6)/3.8	–	0.00(3)	13(5)			

$B_{\text{hf}}$  is the average hyperfine magnetic field and  $\Delta B_{\text{hf}}$  is the width of its distribution, IS is the average isomer shift with respect to  $\alpha\text{-Fe}$  and QS is the average quadrupole splitting. Numbers in parentheses indicate the errors of the least square fit analysis.

value and the pronounced electric field gradient observed for interfacial Fe atoms. In terms of the Mössbauer isomer shift reference data [19], the formation of a wüstite-type oxide at the interface can be excluded – this should be observed as a component with an isomer shift around 1 mm/s. However, IS = 0.4 mm/s, typical for  $\text{Fe}^{3+}$ , is far beyond the metallic Fe value, and indicates a strong modification of the electronic state as compared to the film

centre. This observation is in partial agreement with the conclusion by Luches et al. [10] on the absence of oxide formation at the Fe/MgO(001) interface and its high sharpness. However, this points out that the electronic interaction between Fe and MgO is not negligible. The complex hyperfine pattern seen at the interface at 80 K indicates that the Fe atoms occupied a variety of sites with different coordination and valence states.

At the surface, we observe reduced  $B_{\text{hf}}$  as compared to the film centre (sub-components with  $B_{\text{hf}} = 27.9$  T and  $B_{\text{hf}} = 10$  T, Table 1). In the bulk,  $B_{\text{hf}}$  is a measure of local magnetization but this proportionality fails at surfaces and interfaces. Ohnishi et al. [20] showed theoretically that for the Fe(001) surface, despite the enhancement of the magnetic moment to  $2.98 \mu_B$ , the hyperfine magnetic field is strongly reduced to  $-25.2$  T, and this also holds for the surface layer of 2 Fe monolayers on MgO(001) [2]. Experimentally, the reduction of the surface hyperfine magnetic field was observed only for the closed Fe(110) surface, where the effect is much weaker [21]. For the purpose of the present experiment we have measured *in situ* a CEMS spectrum of a 5 ML  $^{57}\text{Fe}$ (001) layer deposited on a  $^{56}\text{Fe}$ (001) buffer film, which clearly demonstrated surface components with  $B_{\text{hf}} = 25.0$  T and  $B_{\text{hf}} = 7.7$  T and IS very close to that of metallic iron. In our opinion the higher  $B_{\text{hf}}$  represents the ideal surface value, while the smaller one should be attributed to surface defect sites (edge or kink atoms, atoms affected by residual gas adsorption). This measurement strongly supports our interpretations of a hyperfine pattern for the 5 ML Fe film on the cleaved MgO(001) substrate.

We interpret the magnetic transition, which takes place between RT and 80 K, as the onset of a ferromagnetic state

with the film Curie temperature  $T_C$  lying below RT. It roughly agrees with the onset of ferromagnetism at RT for comparable systems that does not fall below  $6 \text{ \AA}$  [11,12]. For Fe films of a similar thickness on metallic substrates  $T_C$  is usually much higher, e.g. a 2 ML Fe(001) film on Au(001) has a  $T_C$  value much greater than 300 K [22]. To our knowledge there is no systematic data for ferromagnetic films on insulators, so it cannot be also excluded that the complex interface structure is responsible for such a low  $T_C$ .

Annealing below 500 K essentially does not influence the CEMS spectra for the cleaved substrate. However, after 1 h annealing at 570 K, the RT spectrum (Fig. 1c) becomes magnetically split. The spectrum could be fitted with broad  $B_{\text{hf}}$  components typical for magnetic fluctuations (spatial or temporal). The shift of the Curie temperature above room temperature must be due to a change in the film morphology from flat to 3-dimensional, which means that annealing caused the continuous Fe layer to break into islands as reported earlier by di Bona et al. [23] for 10 ML Fe films at slightly higher temperatures (above 570 K). The line broadening is probably (at least partially) due to superparamagnetic fluctuations. Estimation of the island size is difficult, because most of the islands are superparamagnetically blocked already at RT,

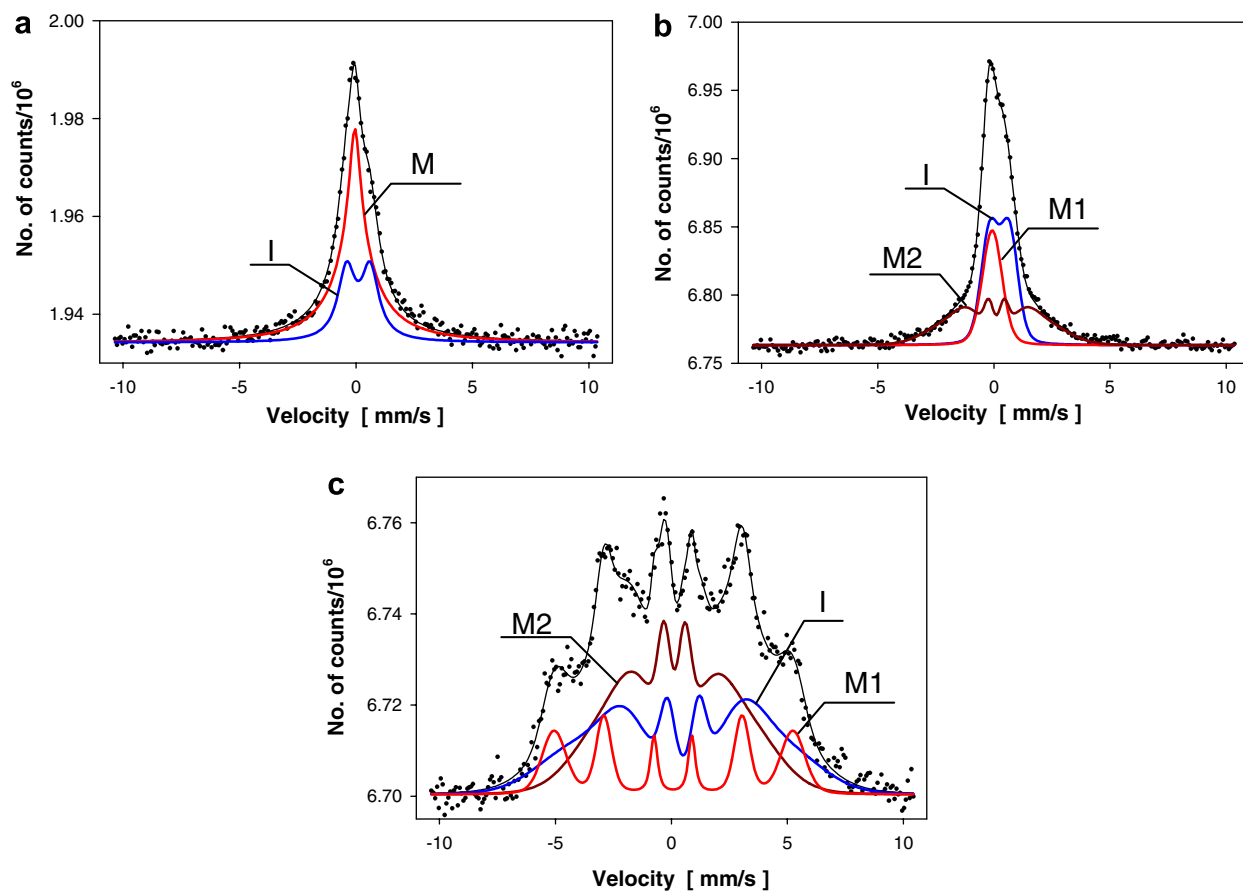


Fig. 2. *In situ* CEMS spectra of 5 ML  $^{57}\text{Fe}$  films on the polished MgO(001) substrate: (a) as prepared, measured at 300 K; (b) and (c) after 1 h annealing at 570 K, measured at 300 K and 80 K, respectively. Symbols that identify the fitted component refer to Table 2.

Table 2  
Fitted hyperfine parameters for 5 nm  $^{57}\text{Fe}(001)$  films on the polished  $\text{MgO}(001)$  substrate

Sample/temperature			IS (mm/s)	$B_{\text{hf}}$ (T)/ $\Delta B_{\text{hf}}$ (T)	QS (mm/s)	Relative intensity (%)
As prepared	300 K	<i>M</i>	0.05(3)	–	–	69(5)
		<i>I</i>	0.20(5)	–	0.51(5)	31(4)
Annealed @ 570 K	300 K	<i>M1</i>	0.03(3)	–	0.00 (1)	23(3)
		<i>M2</i>	0.11(2)	12.9(5)/6	0.00(1)	37(4)
		<i>I</i>	0.35(3)	–	$\pm 0.42(10)$	40(3)
	80 K	<i>M1</i>	0.18(3)	31.9(3)/2.8	0.01(3)	17(3)
		<i>M2</i>	0.25(5)	17.4(7)/9	0.02 (3)	44(3)
		<i>I</i>	0.50(5)	26.4(8)/10	–0.01(3)	39(5)

$B_{\text{hf}}$  is the average hyperfine magnetic field and  $\Delta B_{\text{hf}}$  is the width of its distribution, IS is the average isomer shift with respect to  $\alpha\text{-Fe}$  and QS is the average quadrupole splitting. Numbers in parentheses indicate the errors of the least square fit analysis.

and only the smallest ones contribute to superparamagnetic effects in the CEMS spectra. We can conclude only that, in average, the islands are in a several nanometer size range, in rough agreement with results of Fashold et al. [9]. More reliable analysis was possible based on the 80 K spectrum (Fig. 1d), where the fluctuations are partially suppressed. Beside the metallic (*M1*, IS value of  $\alpha\text{-Fe}$ ) and interfacial/surface (*M2*, broad  $B_{\text{hf}}$  distribution) component, which dominate the spectrum (their intensity corresponds to 90% of the film material), a third component (*I*), with high IS = 0.79 mm/s, can be unambiguously identified. The high isomer shift value ( $\sim 0.7$  mm/s after subtracting the temperature shifts) indicates a strong interaction with the MgO substrate. A half Fe monolayer (as seen from the spectral intensity) forms a magnetically ordered 2-dimensional oxide with iron in the  $\text{Fe}^{2+}$  valence state. Since no systematic studied versus annealing temperature were done, it is not obvious whether the formation of the oxidic state takes place at a certain well defined temperature or develops gradually.

A different growth mode is concluded from the CEMS spectra of the 5 ML Fe film on the polished  $\text{MgO}(001)$  substrate (Fig. 2, Table 2). The room temperature spectrum (Fig. 2a) shows that the metallic-like component (*M*) becomes broadened and its intensity is higher than for the cleaved substrate. The featureless spectrum character means that the film now has a less-ordered structure. In combination with our grazing incidence small angle X-ray scattering data [24], we conclude that the Fe deposit is discontinuous and forms small spherical islands (on average 2 nm diameter, 1 nm height). Apparently, polished substrate defects (contamination, structural defects) influence the nucleation process, leading to the Volmer–Weber growth mode.

The island film structure remains essentially unchanged after annealing. At RT a vast fraction of the Fe atoms do not show long range magnetic order (spectrum in Fig. 2b). The magnetic transition observed between RT and 80 K is now interpreted as the blocking of superparamagnetism of small 3-dimensional clusters. However, the 80 K spectrum after annealing (Fig. 2c) indicates “less” magnetic order than in a similar state of thermal treatment for the cleaved MgO: the structure of the magnetic sextets is unresolved,

there is no the bulk-like component in the spectrum, and the average hyperfine magnetic field  $B_{\text{hf}}$  is smaller than for the film grown on the cleaved substrate (23.4 T and 29.2 T, respectively). As compared to the as-prepared state, the amount of Fe with bulk-like metallic properties (component *M1*) is considerably reduced at the expense of the component *M2* that has a larger isomer shift but smaller  $B_{\text{hf}}$  with broad HFD. This characteristic is typical for interfacial or surface Fe atoms whose fraction increases upon annealing, but without clear indication of oxidation taking place at the Fe/MgO interface (component *I*).

#### 4. Conclusions

The CEMS analysis showed that the 5 ML film on the cleaved substrate is flat and consists of a 2 ML interfacial layer with the electronic structure influenced by the oxide proximity, while the remaining 3 ML are metallic, with the Curie temperature below RT. The annealing changes the film structure only for temperatures above 500 K. In the annealing process the continuous film breaks into 3-dimensional islands and oxidation takes place at the Fe/MgO interface. On the polished substrate, the as-prepared film consists of small superparamagnetic metallic iron particles and annealing up to 570 K does not substantially change the film morphology.

#### Acknowledgments

This work was supported by the European Community under the Specific Targeted Research Project Contract No. NMP4-CT-2003-001516 (DYNASYNC) and by the Polish Ministry of Education and Science. J.K. gratefully acknowledges professorial grant of the Foundation for Polish Science (FNP).

#### References

- [1] C.M. Boubeta, J.L. Costa-Krämer, A. Cebollada, J. Phys.: Condens. Matter 15 (2003) R1123.
- [2] Ch. Li, A.J. Freeman, Phys. Rev. B 43 (1991) 780.
- [3] B.M. Lairson, M.R. Visokay, R. Sinclair, S. Hagstrom, B.M. Clemens, Appl. Phys. Lett. 61 (1992) 1390.
- [4] N. Spiridis, J. Korecki, Appl. Surf. Sci. 141 (1999) 313.

- [5] S.S.P. Parkin, C. Kaiser, A. Panchula, P.M. Rice, B. Hughes, M. Samant, S.H. Yang, *Nature Mater.* 3 (2004) 862;  
S. Yuasa, T. Nagahama, A. Fukushima, Y. Suzuki, K. Ando, *Nature Mater.* 3 (2004) 868.
- [6] T. Urano, T. Kanaji, *J. Phys. Soc. Jpn.* 57 (1988) 3403.
- [7] B.M. Lairson, A.P. Payne, S. Brennan, N.M. Rensing, B.J. Daniels, B.M. Clemens, *J. Appl. Phys.* 78 (1995) 4449.
- [8] T. Suzuki, S. Hishita, K. Oyoshi, R. Souda, *Surf. Sci.* 442 (1999) 291.
- [9] G. Fahsold, A. Pucci, K.-H. Rieder, *Phys. Rev. B* 61 (2000) 8475.
- [10] P. Luches, S. Benedetti, M. Liberati, F. Boscherini, I.I. Pronin, S. Valeri, *Surf. Sci.* 583 (2005) 191.
- [11] Y.Y. Huang, C. Liu, G.P. Felcher, *Phys. Rev. B* 47 (1993) 183.
- [12] J. Dekoster, S. De Groote, T. Kobayashi, G. Langouche, *J. Magn. Mater.* 148 (1995) 93.
- [13] C.M. Boubeta, C. Clavero, J.M. Garcia-Martin, G. Armelles, A. Cebollada, L. Balcells, J.L. Menendez, F. Peiro, A. Cornet, M.F. Toney, *Phys. Rev. B* 71 (2005) 014407.
- [14] M. Sicot, S. Andrieu, F. Bertran, F. Fortuna, *Phys. Rev. B* 72 (2005) 144414.
- [15] K. Thürmer, R. Koch, M. Weber, K.H. Rieder, *Phys. Rev. Lett.* 75 (1995) 1767.
- [16] G. Fahsold, A. Priebe, N. Magg, A. Pucci, *Thin Solid Films* 364 (2000) 177.
- [17] D.G. Rancourt, J.Y. Ping, *Nucl. Instrum. Meth. Phys. Res. B* 58 (1991) 85.
- [18] N.N. Greenwood, T.D. Gibb, *Mössbauer Spectroscopy*, Chapman and Hall, London, 1971.
- [19] J.G. Stevens, *Hyperfine Interact.* 13 (1983) 221.
- [20] S. Ohnishi, A.J. Freeman, M. Weinert, *Phys. Rev. B* 28 (1983) 6741;  
S. Ohnishi, M. Weinert, A.J. Freeman, *Phys. Rev. B* 30 (1984) 36.
- [21] J. Korecki, U. Gradmann, *Phys. Rev. Lett.* 55 (1985) 2491.
- [22] W. Karaś, B. Handke, K. Krop, M. Kubik, T. Ślęzak, N. Spiridis, D. Wilgocka-Ślęzak, J. Korecki, *Phys. Status Solidi (a)* 189 (2002) 287.
- [23] A. di Bona, C. Giovanardi, S. Valeri, *Surf. Sci.* 498 (2002) 193.
- [24] R. Reitingger, et al., *J. Appl. Phys.*, submitted for publication.